ForumAcusticum
2 0 0 5

Modelling of ground vibrations in the vicinity of a tangent railway track

Péter Fiala, János Granát, Fülöp Augusztinovicz
Budapest University of Technology and Economics, H-1117 Budapest, Magyar tudósok körútja 2., Hungary, e-mail: **fiala@hit.bme.hu**

This paper presents a numerical prediction model that allows investigating the wave propagation in horizontally layered soils, in the vicinity of typical urban track systems. The two substructures, i.e. the track system and the soil is modelled separately, using a substructuring method. The track system, consisting of the rail-pair encapsulated in an elastic jacket and embedded in a concrete slab, is modelled as a simple distributed parameter mechanical system. The soil is considered to be a horizontally layered linear elastic domain, the material properties of which are constant within each layer. A boundary integral method using the Green's functions of a layered half-space is used to calculate the soil's stiffness and the contact stresses between the two substructures. This method has the advantage that only the soil-structure interface has to be discretized, and the free surface boundary condition and continuity conditions between the adjacent layers are implicitly satisfied by the fundamental solution. The vibration field around the track system is calculated using the same Green's functions of the layered half-space.

1 Introduction

Ground vibrations generated by surface or underground railway transport can have undesired effect on adjacent buildings and other structures, especially in dense urban areas. Therefore, the ability of predicting train-induced soil vibrations is of high importance.

This paper presents the application of a hybrid numerical model for the modelling of ground vibrations generated by railway traffic. The hybrid numerical model is based on a substructuring method. The whole track model is built up of three sub-structures: i.e. the horizontally layered ground, the homogeneous embankment and the model of the rail–resilient material–sleeper–ballast system. These substructures are handled separately by different modelling techniques. The soil is modelled by a BEM, for the handling of the embankment an analytical and a FEM model is used, and the track system is modelled by means of a method using concentrated and distributed parameter mechanical systems. These models are later coupled in order to obtain a model of the complete track-soil system.

As the investigated frequency range of interest is generally too large for an accurate modelling of the system, a thorough 3D model of the structure cannot be used. Fortunately, the common property of the soil and the embankment – as well as some parts of the track system – is that their geometry is invariant in the x_l longitudinal direction, therefore they can be represented by two-dimensional models. However, as the loads and the resulting displacements vary in the longitudinal direction, a full 2D model cannot be appropriate. This problem can be handled by superposing the loads and responses from spatially harmonic forces and displacements by means of a Fourier transform between the longitudinal direction and the k_l longitudinal wave-number domains. The excitation forces are transformed into the wavenumber-domain, where the relation between the spatially harmonic excitations and responses can be written by means of 2D models, and finally the responses are transformed back to the spatial domain. In the case of simple loads, the excitation can be transformed analytically, the inverse transformation of the response is usually carried out by means of numerical Fourier transformation.

Besides presenting the numerical models, the paper deals with the problem of system identification. The model has been applied to the investigation of vibrations along a suburban train in Budapest. In order to use a proper numerical model, the most important material parameters of the modelled system was determined by dynamic vibration measurements.

2 The numerical prediction model

2.1 The track system

The considered conventional ballasted track is modelled by a simple distributed parameter mechanical system, as shown in Figure 1 [1]. Only symmetrical loads acting on the rail-pair are investigated, therefore the rail-pair is represented by a single beam with given cross sectional area A_r, second moment of inertia I_r, mass density ρ_r, Young-s modulus E_r. The rail's impedance can be expressed in the wavenumber domain as $Z_r(k_l) = k_l^4 E_r I_r - \omega^2 \rho_r A_r$. The rail is connected to a series of concrete sleepers by resilient rail-pads, which are considered as continuous spring-damper system (k_p, c_p). The series of sleepers is characterized by its mass per unit length in the longitudinal direction (m_s). Finally, the sleepers are connected to the embankment by a second continuous spring-damper system (k_b, c_b), representing

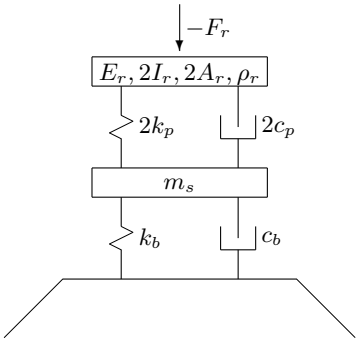

Figure 1: The track model

the ballast.

2.2 Identification of the track parameters

The dynamic parameters of the track system have been identificated by means of impact measurements.

The rail head was excited by a hammer impact above a chosen sleeper, as well as between adjacent sleepers, and the acceleration of the rail head, the sleeper and the embankment below the ballast was measured simultaneously. The obtained FRF-s – the frequency resolution of which is 1 Hz – were smoothed using a five-point moving average technique, and were used as basis functions for a model updating process.

As the attenuation between the accelerations on the rail head and the embankment was always larger than 30 dB, the embankment was considered to be perfectly rigid and motionless during the updating procedure. The geometrical and material parameters of the steel rail and the concrete sleepers were measured in situ or searched from lookup tables. The remaining spring parameters (k_p, c_p, k_b, c_b) were the variables of the updating process.

The displacement of the rail head due to a concentrated point force was calculated in the wavenumber frequency domain, and has been inverse Fourier-transformed to the spatial domain to get the analytical receptance curve of the model. The error function was calculated by integrating the square of the difference between the complex receptance curves, and a Nelder-Mead method [8] has been used for the model updating.

Figure 2 displays the receptance curves obtained by means of measurement and model updating. The updated curve was matched on the first dip and peak of the measured function. In the low frequency range ($f < 40$ Hz) the curves show large deviations, the cause of which is that in this frequency range the flexibility of the embankment cannot be omitted. In the upper frequency range the similarity is satisfactory. The resulting parameter values are: $m_r = \rho_r A_r = 70$ kg/m, $m_s = 400$ kg/m,

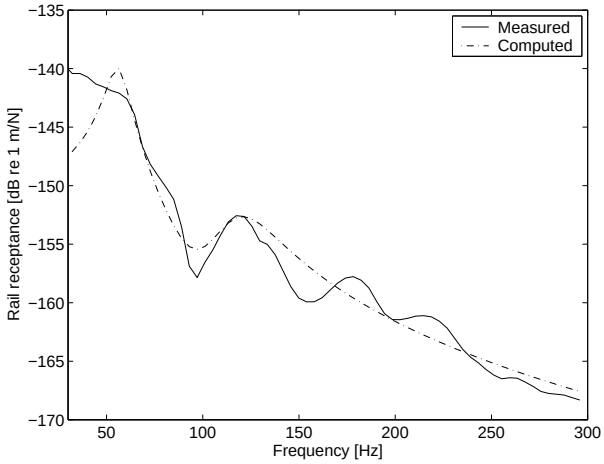

Figure 2: Measured and calculated rail receptance curves

$k_p = 3 \cdot 10^7$ N/m^2, $k_b = 9 \cdot 10^7$ N/m^2, $c_p = 10^4$ Ns/m, $c_b = 6 \cdot 10^4$ Ns/m, $B_r = E_r I_r = 1.17 \cdot 10^7$Nm. All values are projected to a 1 m long section of the track.

2.3 The embankment

As the height of the embankment can be significantly larger than the vibration wavelength even for frequencies lower than 50 Hz, the vibration propagation in the vertical direction has to be taken into account by the embankment model. In this paper two models are investigated.

The dynamical behaviour of the linear embankment domain is governed by the 3D Naver-Cauchy equation:

$$(\lambda + \mu)\nabla_3 \nabla_3 \cdot u + \mu \nabla_3^2 u = -\omega^2 \rho u$$

Applying the assumption that the elements have only nodal displacements in the transverse direction and transforming the equation into the longitudinal wavenumber domain, the

$$(\lambda + \mu)\nabla_2 \nabla_2 \cdot u + \mu \nabla_2^2 u = -(\omega^2 - c_S^2 k_l^2)\rho u$$

equation is obtained, where $c_S = \sqrt{\mu/\rho}$ denotes the shear wave velocity of the domain. Thus, the general 3D problem has been transformed into a series of 2D problems in the wavenumber domain.

The first investigated model applies a conventional FEM algorithm to solve the 2D problems (Figure 3(a)). The second analytical model takes only the vertical displacements of the embankment into account, assumes equally distributed stress in the horizontal direction, and further handles the geometry of the 2D cross section as a bar with exponentially increasing stiffness [2] (Figure 3(b)).

In order to compare the models, the dynamic stiffness of both models has been calculated in the frequency range (the parameters of the models are displayed in table 1).

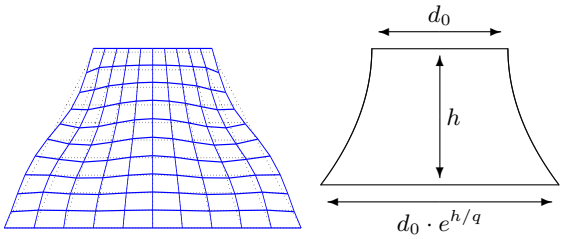

(a) FEM (b) analytical

Figure 3: Different 2D models of the embankment cross section

Table 1: Material parameters of the embankment

ν	$1/3$
ρ	$1300\ \mathrm{kg/m^3}$
c_S	$200\ \mathrm{m/s}$
β	3%
h	$2\ \mathrm{m}$

The models were assumed to rest on a perfectly rigid and motionless plane. The top plane of the FEM model was subjected to rigid body constraint and was assumed to be motionless in the transverse direction. The dynamic stiffness was calculated as the ration of the excitation force and the displacement of the top plane for both models.

The results are plotted in Figure 4 versus real and imaginary frequencies. The imaginary frequency values are relevant, because on the right hand side of equation (2.3) a circular frequency-wavenumber couple can be substituted by a single frequency value $\omega' = \sqrt{\omega^2 - c_s^2 k_l^2}$ that can be pure imaginary, as well as pure real.

Comparing the two models it can be stated that for the case of imaginary frequencies they behave very similarly. For large imaginary frequency values the dynamic stiffness of the embankment increases monotone, meaning that for large k_l wavenumbers the system becomes even stiffer. This is advantageous for the modelling, because it assures that the response won't have large amplitude components in the high wavenumber range, therefore the numerical inverse transformation can be handled easily.

Investigating the real frequency domain, the behaviour of the two systems is similar below 150 Hz In the higher frequency range the simpler bar model shows less resonances and the resonance frequencies are shifted towards smaller frequencies.

2.4 The soil

The soil is assumed to be a horizontally layered elastic medium, characterized by the following material properties: shear modulus G, mass density ρ, Poisson's ratio ν, hysteretic material damping coefficient ξ. These properties are constant within each layer. The whole domain is assumed to be linear, and the soil displacement field is governed by the Navier Cauchy equations of elastodynamics.

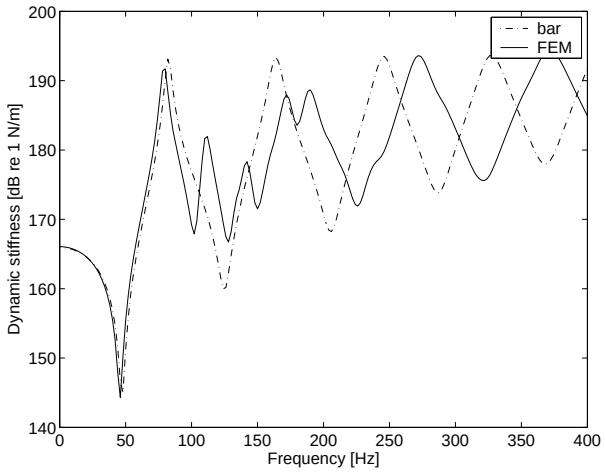

(a) real frequency

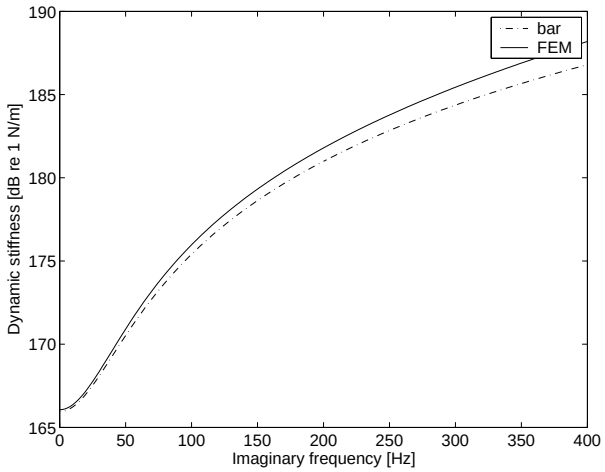

(b) imaginary frequency

Figure 4: Dynamic stiffness of the embankment resting on a rigid support

The stiffness matrix of the soil is calculated by means of a boundary integral method. The $g(x, x_0, \omega, k_l)$ Green's tensors of a layered half-space are used, which give the amplitude of the harmonic wave propagating in the longitudinal direction at the 2D location x if the half-space is loaded by a concentrated harmonic force wave located at x_0. These functions are calculated by means of the direct dynamic stiffness method applied to elastic soil layers in the frequency-wavenumber domain [2, 3, 4].

2.5 SASW testing of the site

In order to measure the material properties of the soil a Spectral Analysis of Surface Waves (SASW) [5, 6] test

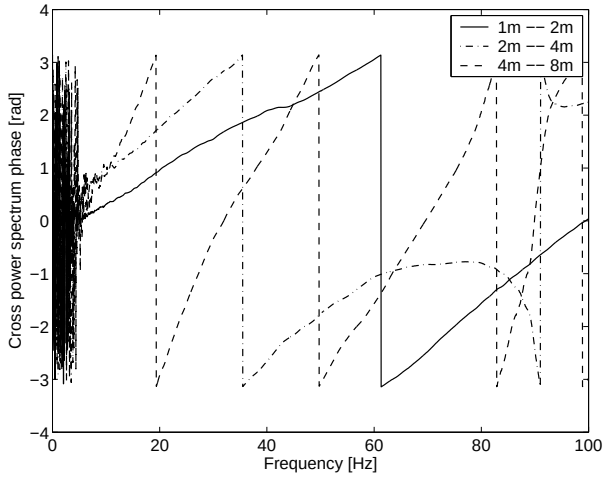

Figure 5: Cross power phase spectra of the adjacent transducers' vibration velocity signals, measured during SASW testing.

has been performed near the test site. The vertical vibration velocity time histories of seven transducers have been measured, while exciting the ground by a falling weight of 80 kg. The transducers have been placed in a common source array, the source-receiver distances varying from 1 m to 32 m, and the vertical vibration velocity time histories have been averaged for a number of 33 impacts.

The experimental dispersion curve of the soil has been determined by calculating the time delay between the adjacent transducers' velocity signals from their velocity cross spectra, which for the first couple of adjacent transducer pairs are shown in Figure 5. As the excited vibrations were very weak below 10 Hz, and the minimal distance between transducers was 1 m, the experimental dispersion curve, shown in figure 6., could be assembled in the frequency interval $f \in [10\text{ Hz}; 60\text{ Hz}]$.

During the inversion procedure the soil layers' material density and Poisson's ratio was assumed to be constant within the layers. By adjusting the Shear modulus and width of two layers lying on an infinite half-space, the soil profile given in table 2. was obtained.

The hysteretic material damping ratio of the soil was estimated from the attenuation curves measured during the SASW testing. The estimation procedure was carried out by modelling the falling weight as a uniform traction acting on a disk of radius 0.1 m on the soil surface. The vibration levels at the location of the transducers have been calculated in the wavenumber domain, by means of the direct dynamic stiffness matrix method, followed by an inverse Hankel transform. A damping value of $\beta = 3\ \%$ gave appropriate results: the deviation between the measured and modelled attenuation values is less than $1 - 2$ dB.

Table 2: Material properties of the soil layers, obtained by SASW testing

	width [m]	c_S $[m/s]$	ρ [kg/m^3]	ν	β
layer 1.	2.2	135	1700	$1/3$	3 %
layer 2.	2.8	175	1700	$1/3$	3 %
half-space	∞	340	1700	$1/3$	3 %

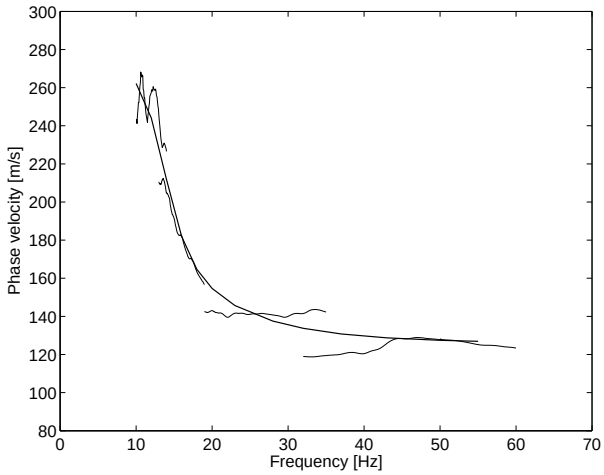

Figure 6: The experimental and theoretical dispersion curves

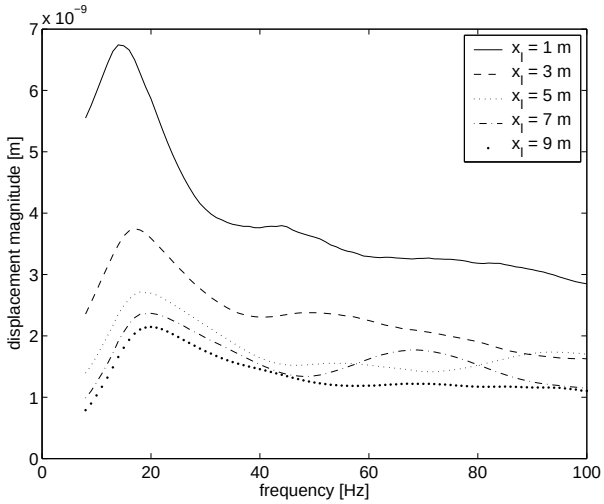

Figure 7: Magnitude spectra of soil displacement along the soil-embankment interface, due to a concentrated force acting on the soil surface, in the absence of the embankment

2.6 modelling results

Figure 7 displays some modelling results of the soil domain. The soil-embankment interface has been excited by a unit vertical point force, and the surface displacement in the absence of the embankment has been calculated along the interface, in several positions. The figure displays the obtained spectra for five different positions. It can be observed that the layering of the soil causes resonances because of the reflection of vibration waves from the boundary of adjacent layers. A common resonance frequency at approx. 15 Hz can be observed on each curve, the higher frequency resonances vary more with distance.

3 Modelling results for the complete system

In the following parts of the paper the modelling results for the total coupled structure will be presented. In this phase the material properties of the embankment were assumed to be identical with those of the upper soil layer. As the simplest case, the response due to a still harmonic vertical impact force on the rail-head was investigated at several positions: on the rail-head, at the sleepers, on the top of the embankment and along the soil-embankment interface.

Figure 8 displays the obtained displacements in the longitudinal wavenumber-frequency domain. On both subfigures the magnitude of the displacement is plotted versus nondimensionalized wavenumber and frequency. The nondimensionalized wavenumber is calculated by dividing the longitudinal wavenumber by the k_S^L shear-wave wavenumber of the upper soil layer (or the embankment), $k_S^L = \omega / c_S^L$.

These wavenumber-frequency spectra are useful, because they allow us to get information about the velocity of vibration propagation in the longitudinal direction, as at a given frequency the longitudinal velocity can be calculated as $c_l = \omega / k_l$.

For the case of the rail-head (Figure 8(a)), it can be seen that the dominant zones of the wavenumber-frequency spectrum are positioned in the frequency range $f \geq 40$ Hz, and above 50 Hz the longitudinal vibration velocity increases linearly with frequency. This can be obtained finding that the peak in the figure doesn't vary with frequency in the upper frequency range, and the wavenumber scale is nondimensionalized by the quantity ω / c_S.

For the case of the soil-embankment interface (Figure 8(b)) the spectrum is shifted towards low wavenumber values, meaning that the vibration propagation velocity is very large in the longitudinal direction. This means that the points of the soil-embankment interface move almost together along the longitudinal direction, so the wave-propagation is dominant in the direction perpendicular to the longitudinal. Other interesting phenomenon is that the levels of vibration are more than a magnitude smaller on the soil than on the rail-head, which is mainly due to the damping behaviour of the resilient material and somewhat due to the hysteretic losses in the 2 metres high embankment.

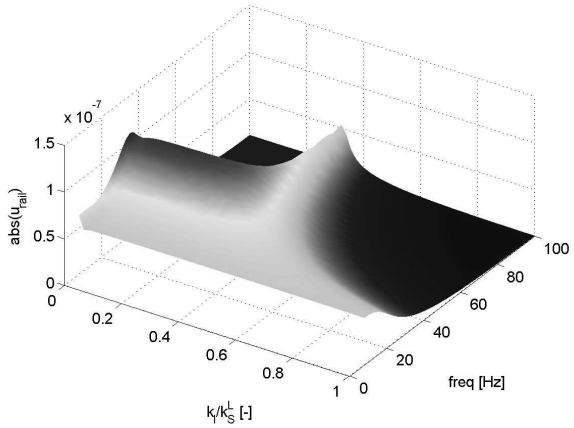

(a) on the rail-head

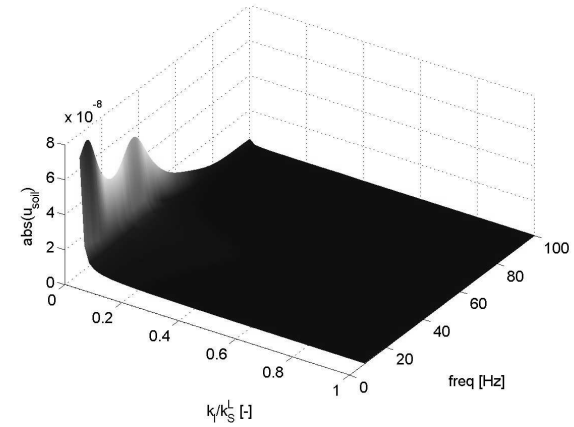

(b) on the soil-embankment interface

Figure 8: Displacements of the rail and the soil in the wavenumber-frequency domain

These displacement spectra have been transformed to the spatial domain in order to get impulse spatial responses, i.e. response spectra due to a symmetric hammer impact on the rail-head. These spectra have been calculated for several x_l longitudinal positions. Here the spectra obtained for $x_l = 1$ are presented in Figure 3.

It can be observed that the basic behaviour of the whole system is determined by the lover resonance frequency of the rail-sleeper-ballast system, as showed by the first large peak at approx. 40 Hz at each curves. An interesting phenomenon is that the four curves corresponding to

the rail-head, the sleeper, the top of the embankment and the embankment-soil interface can be divided into two groups, the elements of which show very similar behaviour, meaning that the ballast has a greater influence on the vibration attenuation than the embankment.

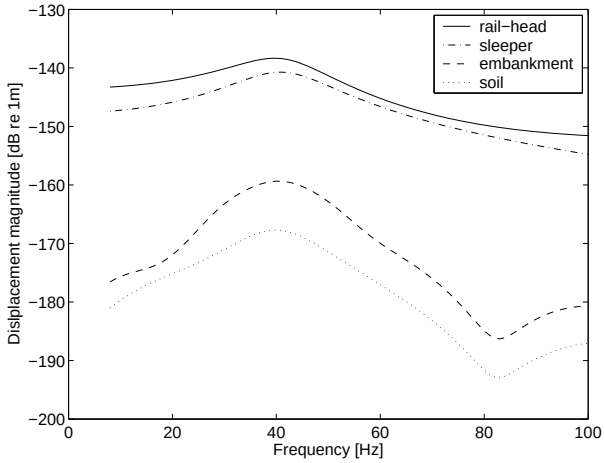

4 Summary

The application of a hybrid method for the modelling of vibrations along a tangent track system has been presented. Several methods have been used and presented to identify the material properties of the different model components by means of vibration measurements. The application of the SASW method proved to be appropriate for the determination of soil properties, while the track parameters could be determined by means of simple impact measurements on the track. The application of the model on the whole coupled structure made it possible to determine the vibration levels at different points under the excitation force along the track and to determine the basic directions of vibration propagation near the structure.

References

[1] V.I. Markine, A.P. De Man, C. Esveld, Identification of Dynamic Properties of a Railway Track *Proc. IUTAM Symposium on Field Analyses for Determination of Material Parameters Experimental and Numerical Aspects Sweden*, July 31st - August 4th, 2000.

[2] Wolf, J.P., *Dynamic Soil-Structure Interaction*, Prentice Hall Inc., New Jersey, 1985.

[3] Apsel, R. and Luco, J.E., On the Green's functions of a layered half-space, part II. *Bulletin of the Seismological Society of America*, 73(4), pp.931-51, 1983.

[4] Auersch, L., Wave propagation in layered soils: Theoretical solution in wavenumber domain and experimental results of hammer and railway traffic excitation. *Journal of Sound and Vibration*, 173(2):233-64. 1994.

[5] Carlo G. Lai, Glenn J Rix, *Simultaneous inversion of Rayleigh Phase Velocity and Attenuation for Near-Structure Site Characterization* research report, Georgia Institute of Technology, School of Civil and Environmental Engineering, 1998.

[6] N. Gucunski, V. Ganji, M.H.Maher, Effects of Obstacles on Rayleigh Wave Dispersion obtained from the SASW test, *Soil Dynamics and Earthquake Engineering*, 15(1996) pp.223-31, 1996.

[7] L. Chen, J. Zhu, X. Yan, C. Song, On arrangement of source and receivers in SASW testing, *Soil Dynamics and Earthquake Engineering*, 24(2004) pp.389-96, 2004.

[8] J.H. Matthews, K.K. Fink, *Numerical Methods Using Matlab, 4-th edition*, Prentice-Hall inc., New Jersey, USA, 2004.